

## The effect of wind mixing on the vertical distribution of buoyant plastic debris

T. Kukulka,<sup>1</sup> G. Proskurowski,<sup>2,3</sup> S. Morét-Ferguson,<sup>2</sup> D. W. Meyer,<sup>2,4</sup> and K. L. Law<sup>2</sup>

Received 27 January 2012; revised 5 March 2012; accepted 7 March 2012; published 3 April 2012.

[1] Micro-plastic marine debris is widely distributed in vast regions of the subtropical gyres and has emerged as a major open ocean pollutant. The fate and transport of plastic marine debris is governed by poorly understood geophysical processes, such as ocean mixing within the surface boundary layer. Based on profile observations and a one-dimensional column model, we demonstrate that plastic debris is vertically distributed within the upper water column due to wind-driven mixing. These results suggest that total oceanic plastics concentrations are significantly underestimated by traditional surface measurements, requiring a reinterpretation of existing plastic marine debris data sets. A geophysical approach must be taken in order to properly quantify and manage this form of marine pollution. **Citation:** Kukulka, T., G. Proskurowski, S. Morét-Ferguson, D. W. Meyer, and K. L. Law (2012), The effect of wind mixing on the vertical distribution of buoyant plastic debris, *Geophys. Res. Lett.*, 39, L07601, doi:10.1029/2012GL051116.

### 1. Introduction

[2] Since the introduction and popularization of “engineered thermoplastics” in the 1950s, plastic has become one of the world’s most important and widespread commodities. The same engineered properties that contribute to the enormous utility of plastic, namely durability and resistance to degradation, also result in long residence times (decades to millennia) when plastic is introduced into the natural environment [Andrady, 2011]. While plastic marine debris has been identified as an open ocean pollutant since the 1970s in the North Atlantic [Carpenter and Smith, 1972; Colton et al., 1974; Wilber, 1987] and North Pacific [Day and Shaw, 1987; Wong et al., 1974], only recently has the spatial and temporal scope of plastic pollution in surface open ocean environments been thoroughly detailed [Law et al., 2010]. The multi-decadal observations of plastic based on surface plankton net tow measurements in the western North Atlantic basin presented by Law et al. [2010] validate a surface drifter data-driven model [International Pacific Research Center, 2008; Maximenko et al., 2009] that predicts a region of plastic accumulation spanning millions of square kilometers in the

central North Atlantic. The observations and model predictions in the North Atlantic clearly show that plastic is most highly concentrated within the large-scale subtropical convergence of the surface velocity field created by the wind-driven Ekman currents and geostrophic circulation [Law et al., 2010]. Despite an increasing public awareness of ocean plastic, the abundance, distribution, and temporal and spatial variability of this contaminant are still poorly constrained; however, it is clear that plastic particles are a global ocean phenomenon [Barnes et al., 2009].

[3] The known environmental impacts of ocean plastic are extensive [Sudhakar et al., 2008] and include: entanglement of marine fauna [Laist, 1987]; ingestion by seabirds [Titmus and Hyrenbach, 2011], mesopelagic fish [Davison and Asch, 2011], planktonic organisms and marine mammals [Laist, 1987; Thompson et al., 2004]; provision of protected substrates on which microbial and colonizing species thrive and are dispersed to potentially non-native waters [Barnes and Milner, 2005; Webb et al., 2009]; and concentration and transport of organic contaminants to marine organisms at multiple trophic levels [Mato et al., 2001; Teuten et al., 2007, 2009].

[4] The most abundant form of plastic marine debris in the surface open ocean is millimeter-sized fragments of consumer plastics with an average material density of  $965 \text{ kg m}^{-3}$  (e.g., low- and high-density polyethylene, polypropylene, and foam polystyrene) that is less than the surface seawater density of  $1027 \text{ kg m}^{-3}$  [Morét-Ferguson et al., 2010]. As a passive particle, this plastic debris is subject to the physics of mixing within the ocean surface boundary layer. We hypothesize that the buoyant upward flux of plastic pieces is balanced by a turbulent downward flux for moderate wind conditions, resulting in vertically-distributed plastic debris throughout the surface wind-mixed layer.

[5] Here we show, from subsurface observations and a one-dimensional theoretical model, that wind stress results in the vertical mixing of buoyant plastic debris into the surface mixed layer and that, depending on wind speed, surface measurements may underestimate the total amount of buoyant plastic distributed in the upper water column by up to a factor of 27. Finally, the integrated plastic concentration from the surface to the base of the wind-mixed layer is estimated with the model for a given surface plastic concentration and wind speed. This type of geophysical approach is necessary in order to properly quantify plastic marine debris pollution.

### 2. Observations

#### 2.1. Surface Tows

[6] The plastic data presented here are a subset of the Law et al. [2010] dataset, for which there exists a robust record of

<sup>1</sup>School of Marine Science and Policy, College of Earth, Ocean, and Environment, University of Delaware, Newark, Delaware, USA.

<sup>2</sup>Sea Education Association, Woods Hole, Massachusetts, USA.

<sup>3</sup>School of Oceanography, University of Washington, Seattle, Washington, USA.

<sup>4</sup>Marine Science Department, Eckerd College, St. Petersburg, Florida, USA.

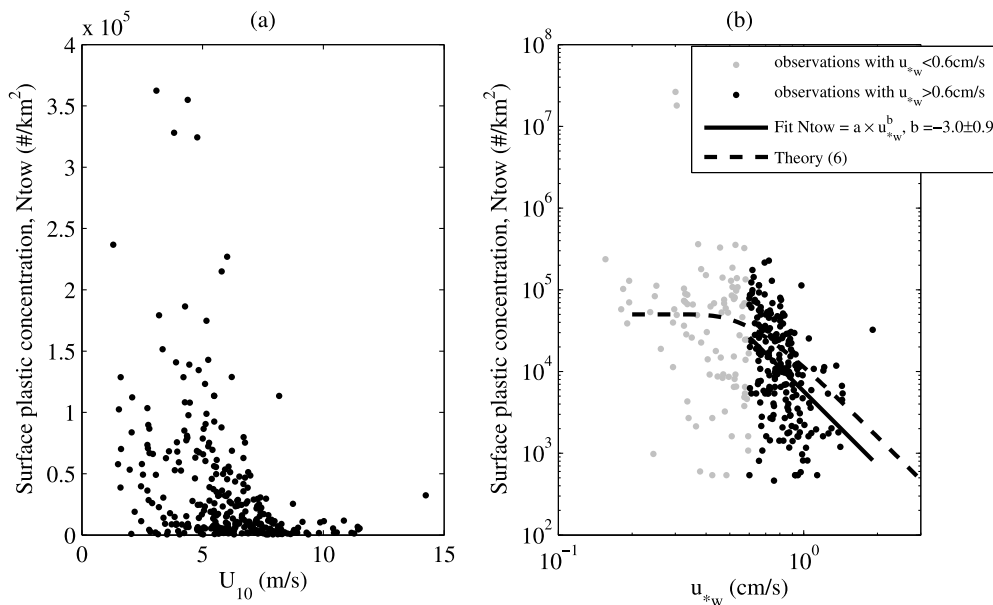


**Figure 1.** Measured surface plastic concentration ( $N_{\text{tow}}$ ) versus (a) wind speed,  $u_{10}$  and (b) water friction velocity,  $u_{*w}$ , for  $u_{*w} > 0.6$  cm/s (black dots) and  $u_{*w} < 0.6$  cm/s (gray dots). The best fit line is for observations with  $u_{*w} > 0.6$  cm/s, when wind effects are expected to be significant according to the discussion in section 3.2 (solid line). The theoretical estimate is based on (5) with (3) and  $N = 5 \times 10^4$  (#/km<sup>2</sup>) (dashed line). In Figure 1a the two largest plastic concentration values occurring at  $u_{10} = 2.5$  m/s are not shown.

wind velocity during sampling activities. Since the early 1980s, Sea Education Association (SEA) has conducted plastic marine debris research on annually-repeated cruise tracks in the western North Atlantic. The results of more than 6100 net tows conducted on  $\sim 170$  SEA expeditions indicate that a region of high plastic concentration exists between 22° and 38°N latitude in the western North Atlantic [Law *et al.*, 2010]. The subset analyzed here includes data from 343 net tows since 2003, when a scientific meteorology package was installed on SEA vessels. Only net tows occurring within the high plastic concentration region (22–38°N) were considered for this study.

[7] Surface (neuston) net tows follow a standardized protocol used for more than 25 years at SEA. The 335  $\mu\text{m}$  mesh net has a  $0.5 \times 1.0$  meter opening (on average 0.25 m of the net opening is submerged), and is towed at a ship speed of  $\sim 2$  knots for 30 minutes. Thus, tows are nominally 1 nautical mile (1.85 km) long, with actual tow lengths determined from GPS position data, hull-based inductive log, and net-based flow-meter readings. Once the sample is aboard, the plastic is hand-separated from the biomass, then enumerated, air-dried and archived. Here we report observed plastic concentration as the number of plastic pieces divided by the tow area, in units of #/km<sup>2</sup> ( $N_{\text{tow}}$ ). For volumetric comparisons, we assume the volume of the tow to be 0.25 m multiplied by the tow area.

[8] Wind velocity was derived from shipboard anemometer measurements at 31 m height above the mean waterline. The bulk aerodynamic formulae of Large and Pond [1981] and the log-profile assumption (buoyancy effects were negligible) were used to calculate wind velocity at height 10 m above the sea surface ( $u_{10}$ ) and frictional velocity of water ( $u_{*w} = [\tau/\rho_w]^{1/2}$ , where  $\tau$  is the wind stress and  $\rho_w$  is the

density of water). For reference, a true wind speed of 10 knots measured at 31 m is equivalent to  $u_{10} = 4.7$  m/s and  $u_{*w} = 0.55$  cm/s. Wind parameters were calculated from instantaneous measurements of true wind speed, then averaged over the duration of each plankton net tow.

[9] Observations show that high plastic concentrations ( $> 5 \times 10^4$  pieces/km<sup>2</sup>) were measured only at low wind speeds (Figure 1a). Despite the substantial scatter due to the large spatial variability in plastic concentration, a linear regression relating concentration to wind forcing ( $N_{\text{tow}} = a (u_{*w})^b$ ) gives an inverse relationship with  $b = -1.6 \pm 0.4$  (95% confidence interval), indicating that lower surface concentrations tend to be associated with higher wind speeds. Guided by the theory developed below, we also computed the regression coefficients for  $u_{*w} > 0.6$  cm/s, giving  $b = -3.0 \pm 0.9$  (95% confidence interval) (Figure 1b). We suggest the inverse relationship observed in the data results from turbulent wind mixing that distributes the plastic particles throughout the surface boundary layer. This hypothesis is supported by our subsurface observations of plastic concentration.

## 2.2. Subsurface Tows

[10] In June–July 2010, a series of 12 surface and subsurface net tows were conducted to investigate the amount of plastic in the upper water column of the North Atlantic subtropical gyre between 29–31°N and 40–54°W. At each sampling location a CTD profile was first used to determine the depth of the mixed layer based on a temperature threshold [de Boyer Montegut *et al.*, 2004]. Then a surface net tow was accompanied by a set of net tows at discrete depths within the mixed layer (typically  $\sim 5$ , 10, and 20 m; Figure 2). The subsurface net tows were conducted using a

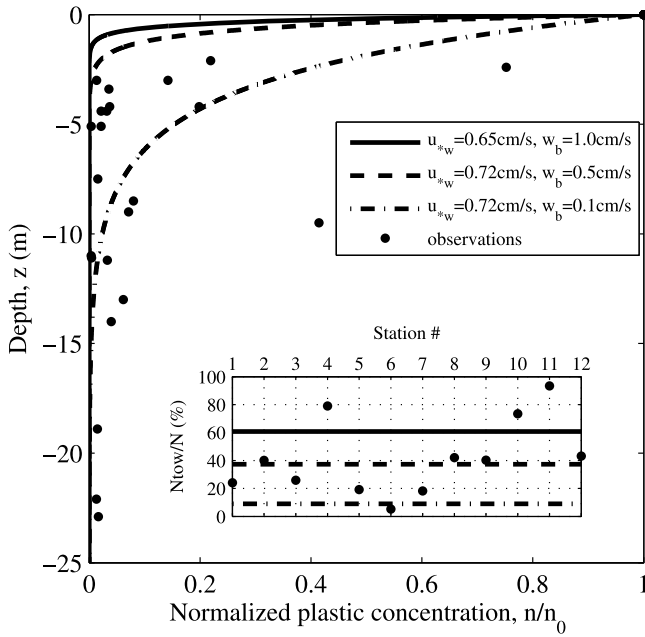


**Figure 2.** Observed (dots) and modeled (lines) depth profiles of plastic concentration, normalized by the surface value. Typical values are  $u_{*w} = 0.65$  cm/s (observed during profile measurements) and  $w_b = 1$  cm/s (laboratory observations). While varying  $u_{*w}$  within the observed range (0.60–0.72 cm/s) does not significantly alter the model profile, there is a strong dependence on  $w_b$ . The inset shows estimates of surface plastic concentration relative to total plastic concentration ( $N_{\text{tow}}/N$ ) from conservatively interpolated profile observations (dots) and model results (lines).

modified Aquatic Research Instruments multiple-net Tucker Trawl [Hopkins *et al.*, 1973], a messenger-operated closing net that allows a specific depth layer to be sampled without contamination from the surface or the down- and up-cast portions of the tow. The assembly was equipped with a CTD and flow-meter to measure the tow depth and volume sampled, respectively. Subsurface plastic concentrations are reported as pieces per unit volume and normalized using the concurrent surface concentration to facilitate comparison of depth profiles (Figure 2). The sampling was conducted under nearly uniform wind conditions of 11–13 knots ( $u_{*w} = 0.60$ – $0.72$  cm/s).

[11] Eighty-one percent (26/32) of subsurface net tows contained plastic (Figure 2). Thus, plastic is not simply surface-trapped, but is vertically distributed within the mixed layer. To estimate the total amount of plastic in the surface mixed layer from observations at three or four discrete depths, a “stair step” depth profile was computed with a constant value for each “step” being equal to the observation at the base of that step. Because plastic concentration typically decreases with depth, this conservative estimate likely underestimates the total plastic in each step. The resulting profile was then vertically integrated and used to estimate the fractional concentration represented by the surface measurement, which ranged from 6% to 94% of total plastic concentration with an average of 42% (Figure 2, inset). Thus, a surface measurement alone does not

accurately represent the amount of plastic in the near-surface layer.

[12] Because of the near-uniform wind conditions during sampling, we could not establish a relationship between the vertical distribution of plastic and strength of wind forcing. However, despite consistent wind conditions the vertical distribution of plastic was variable. Such behavior could result from differences in plastic properties (e.g., variable density and shape resulting in different rise velocities); mixed layer depth; wave-induced mixing due to breaking waves or Langmuir circulations, which depends on the sea state; and variability in total plastic concentration.

### 3. Model

#### 3.1. Basic Physics

[13] We decompose  $n$ , the instantaneous number of plastic pieces per unit volume, into the horizontal average,  $\bar{n}$ , and the deviation from the horizontal average,  $n'$ , where  $n = \bar{n} + n'$ . The horizontally-averaged vertical transport of plastic pieces through the water column at depth,  $z$ , is governed by a buoyant upward flux,  $-w_b \bar{n}$ , and a Reynolds-averaged flux,  $-\overline{wn'}$ , where  $w_b$  is the buoyant rise velocity and  $w$  is the vertical turbulent velocity. Without net fluxes through the boundaries (no plastic input at the air-sea interface or mixed layer base), the conservation of plastic pieces in steady state imposes:

$$-w_b \bar{n} - \overline{wn'} = 0. \quad (1)$$

Preliminary laboratory experiments on a small subset of archived North Atlantic plastic samples in quiescent water indicate that the rise speed of plastic pieces ranges from  $w_b = 0.005$  to  $0.035$  m/s. Flat-shaped fragments, which represent the most abundant form of plastic marine debris [Morét-Ferguson *et al.*, 2010], appear to have a smaller average rise speed,  $w_b = 0.014 \pm 0.007$  m/s (average  $\pm$  standard deviation). For simplicity we assumed  $w_b = 0.01$  m/s by default, understanding that the rise speed depends on plastic size, shape, and density, as well as water turbulence that may cause additional lift and drag forces [e.g., Guha, 2008]. Below we discuss the sensitivity of our results on rise speed.

[14] A solution for  $\bar{n}$  is obtained by parameterizing the turbulent flux via an eddy viscosity turbulence model:

$$-\overline{wn'} = A \frac{d\bar{n}}{dz}. \quad (2)$$

The turbulent (eddy) exchange coefficient,  $A$ , depends on  $z$ , reflecting depth variations in turbulence characteristics [Large *et al.*, 1994]. To examine whether turbulent mixing near the air-sea interface is strong enough to mix down the buoyant plastic pieces, we introduce  $A_0$  as a scale for the near-surface  $A$ . The vertical length scale for the decay of  $\bar{n}$  is  $A_0/w_b$ , so that for  $A_0/w_b \geq O(d)$ , plastic pieces are mixed below the immersion depth of the surface-towed net,  $d = 0.25$  m. For  $A_0/w_b \gg d$  only a small fraction of plastic pieces is captured in the net, while for  $A_0/w_b \ll d$  all pieces are captured.

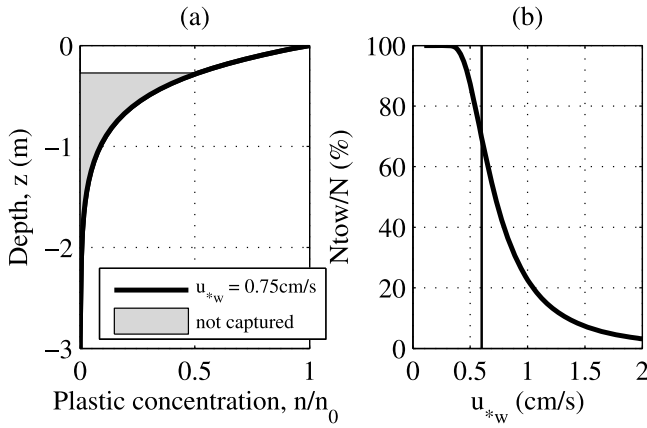


**Figure 3.** (a) Theoretical volumetric plastic concentration  $\bar{n}(z)$  normalized by its surface value  $\bar{n}_0$  according to (4) for average wind conditions ( $u_{*w} = 0.75$  cm/s). More than 54% of plastic pieces are below the surface tow measurement (gray area). (b) Theoretical fraction of surface-captured plastic pieces normalized by the total number ( $N_{\text{tow}}/N$ ) as function of water friction velocity according to (5). The wind stress effect becomes significant for  $u_{*w} > 0.6$  cm/s ( $u_{10} \sim 4.5$  m/s, wind speed  $\sim 9$  knots).

### 3.2. Near-Surface Turbulent Mixing and Solutions

[15] For moderate and high wind conditions, breaking surface waves and Langmuir circulations control mixing near the air-sea interface [Melville, 1996; Thorpe et al., 2003]. To model relatively strong near-surface mixing due to breaking waves, we adopt an empirical parameterization [Thorpe et al., 2003]

$$A_0 = 1.5u_{*w}\kappa H_s \quad (3)$$

for  $z > -1.5 H_s$ , where  $\kappa = 0.4$  is the von Karman constant and  $H_s$  is significant wave height.  $H_s$  is parameterized by  $H_s = 0.96 g^{-1} \sigma^{3/2} u_{*a}^2$  [Csanady, 2001; Thorpe et al., 2003] where  $g = 9.81$  m/s<sup>2</sup> is the acceleration of gravity,  $\sigma = c_p/u_{*a}$  denotes the wave age,  $c_p$  is the phase speed of the dominant wave, and  $u_{*a}$  is the frictional air velocity (derived from true wind speed). Because the wave field was not directly measured and winds were relatively steady and unidirectional, we assume a fully developed sea with  $\sigma = 35$  [Komen et al., 1996]. For this wave age, the critical threshold water friction velocity is  $u_{*c} = 0.6$  cm/s when  $A_0 = w_b d$ , so that wind stress effects are expected to be significant for  $u_{*w} > u_{*c}$  (equivalent to  $u_{10} > 5$  m/s). Note that because for average conditions the vertical decay length scale,  $A_0/w_b$  ( $\sim 0.4$  m), is much smaller than the typical mixed layer depth ( $\sim 25$  m), the mixed layer depth is negligible in this scenario. For high wind conditions and relatively shallow mixed layers, the mixed layer depth may become important.

[16] Given the boundary condition  $\bar{n}_0 = \bar{n}(z = 0)$ , the near surface solution of (1) and (2) is

$$\bar{n}(z) = \bar{n}_0 \exp(zw_b A_0^{-1}) \quad (4)$$

The model indicates that for average observed wind conditions ( $u_{*w} = 0.75$  cm/s in this study), 54% of plastic pieces are mixed below the tow depth and thus are not captured by

the surface measurement (Figure 3a). The horizontally-averaged total number of plastic pieces per unit surface area is  $N = \int_{-\infty}^0 \bar{n} dz$ , so that the relation between  $N$  and the observed surface value,  $N_{\text{tow}}$ , is expressed as

$$N_{\text{tow}} = \int_{-d}^0 \bar{n} dz \approx N [1 - \exp(-dw_b A_0^{-1})]. \quad (5)$$

Here we have extended the near-surface solution to depth  $d$ , which is approximately valid because  $\bar{n}$  decays rapidly with depth for typical wind conditions. For  $u_{*w} > u_{*c}$ ,  $N_{\text{tow}}/N$  strongly decreases with increasing  $u_{*w}$  (Figure 3b), consistent with the above scaling arguments. For  $u_{*w} \ll u_{*c}$ , surface values approach  $N_{\text{tow}} \rightarrow N$ , while for  $u_{*w} \gg u_{*c}$ , with (3) and a constant wave age, one obtains

$$N_{\text{tow}}/N \approx dw_b/A_0 \propto u_{*w}^{-3}. \quad (6)$$

### 3.3. Comparison With Observations

[17] The dependence of surface plastic concentration ( $N_{\text{tow}}$ ) on wind forcing ( $u_{*w}$ ) is consistent between the model ( $b = -3$  in (6)) and the observations ( $b = -3.0 \pm 0.9$ ; Figure 1b). Furthermore, the increase in  $b$  with increasing  $u_{*w}$  in the model ( $b = 0$  for  $u_{*w} \ll u_{*c}$ , and  $b = -3$  for  $u_{*w} \gg u_{*c}$ ) is consistent with observations. The comparison between observed depth profiles of plastic concentration and model estimates (Figure 2) is incomplete because the theory predicts the largest decrease in the upper two meters (compare with Figure 3a) where no subsurface measurements exist. Furthermore, comparison is limited because profiles were obtained in nearly constant wind conditions. At greater depths the model generally underestimates the observed plastic content (Figure 2); in observational depth profiles the surface value represents, on average, 42% of the total plastic content in the sampled layer (Figure 2, inset), while in the model the average is 61%. This discrepancy may result from variable plastic properties and associated rise speeds (e.g., model results with smaller rise speeds agree better with measured plastic concentrations at depth), as well as turbulence unaccounted for in the model. Another important factor is enhanced vertical near-surface transport due to Langmuir circulation (LC), which influences the vertical distribution of buoyant material such as oil droplets [e.g., D'Asaro, 2000] or air bubbles [e.g., Thorpe et al., 2003], but which is challenging to capture in a simple one-dimensional column model [Kantha and Clayson, 2004; Kukulka et al., 2009; Li et al., 1995; McWilliams and Sullivan, 2000; Smith, 1992; Smyth et al., 2002]. In this case, it may be more physical to relate the mixing length in (3) to the mixed layer depth. Idealized LC models suggest that buoyant particles can be trapped near downwelling regions [Stommel, 1949] and three-dimensional turbulence-resolving simulations of buoyant particles indicate that the LC effect is indeed important [Skylingstad, 2003; T. Kukulka et al., submitted to *Journal of Geophysical Research*, Langmuir Circulation in a coastal ocean, 2012]. Clearly, a more comprehensive model must take into account variable sea state with associated wave

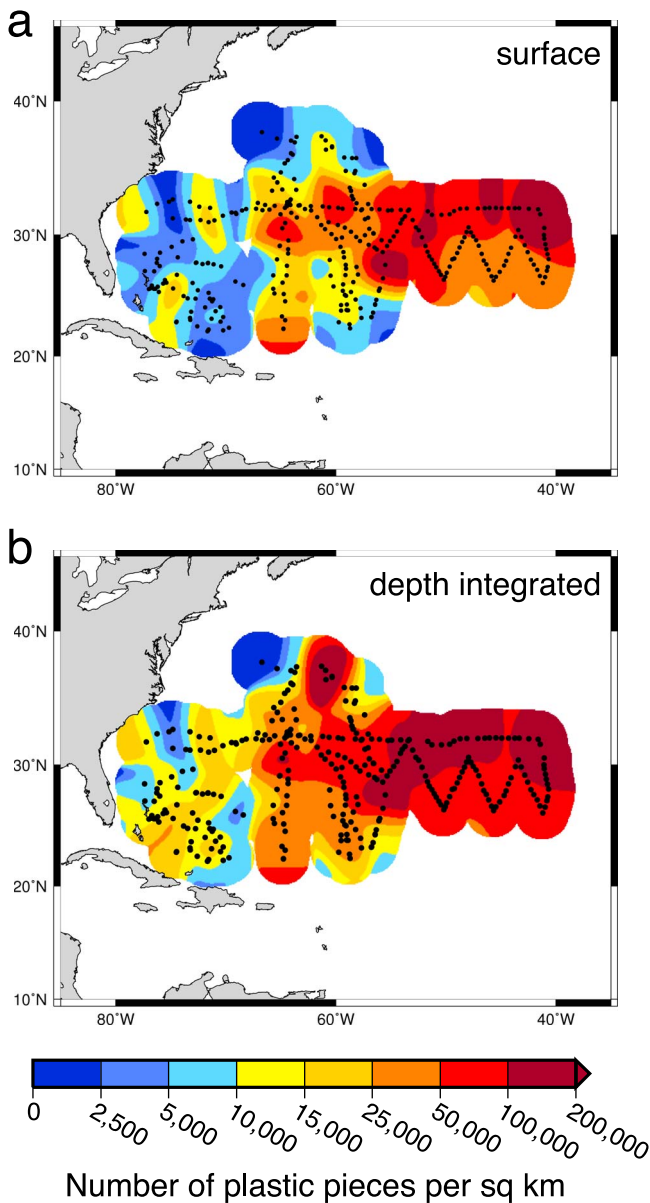


**Figure 4.** Spatially-averaged plastic concentration as determined from (a) 343 surface net tow measurements and (b) vertically-integrated plastics content from model calculations using surface net tow measurements and concurrently measured wind speed. In high wind conditions ( $u_{10} > 12$  m/s) model estimates were up to 27 times the surface observations. Maps were processed identically by averaging over  $0.5^\circ$  bins, smoothing with a 500 km width Gaussian filter, and masking at 200 km from the nearest data point using Generic Mapping Tools [Wessel and Smith, 1998].

mixing (LC and breaking waves) as well as the variability of observed plastic properties.

#### 4. Total Plastic Content Taking Wind Mixing Into Account

[18] Surface net tows cannot account for the total amount of plastic pieces in the upper ocean mixed layer, except in low wind conditions ( $u_{10} < 5$  m/s). However, when surface

net tow data are combined with wind speed observations, it is possible to improve the estimate of the total amount of plastic in the wind-mixed surface layer using the model presented here. Using collocated observations of surface plastic concentration and wind speed as inputs to the model, equation (5) yields the depth-integrated plastic concentration. Figure 4b illustrates this improved estimation of plastic concentration in the subtropical North Atlantic, relative to measured values (Figure 4a). The model predicts an average integrated concentration 2.5 times the measured surface value, with a maximum of 27 times the surface value. As noted above, this model likely underestimates the wind mixing effect and therefore total plastic content, thus actual integrated concentrations in the subtropical North Atlantic could be much higher.

#### 5. Conclusions

[19] Based on surface and subsurface observations and a one-dimensional column model, we have illustrated that plastic concentrations measured using surface tow measurements depend on wind speed (tows in high wind conditions tend to capture fewer plastic pieces) because plastic pieces are vertically distributed in the mixed layer due to wind-induced mixing. Using subsurface depth profiles of plastic concentration and a theoretical model, we show that surface tow measurements significantly underestimate the total plastic content even for moderate wind conditions. Therefore, accurate estimates of total plastic content in the upper ocean must take into account the effects of wind-driven mixing.

[20] **Acknowledgments.** TK was supported by startup funds from the School Marine Science and Policy, University of Delaware. Philip Orton provided valuable comments on an earlier draft. Shipboard profile observations were supported in part by NFWF-NOAA Marine Debris Program Award 2009-0062-002 on the Plastics at SEA: North Atlantic Expedition 2010. The authors would like to thank the multitude of SEA students, scientists and crew involved in the collection and processing of marine plastic debris samples over the past two decades. We would like to thank two anonymous reviewers for constructive criticism that improved the paper. Authors Tobias Kukulka and Giora Proskurowski (email: giora@uw.edu) are equally contributing authors and both are corresponding authors.

[21] The Editor thanks two anonymous reviewers for their assistance in evaluating this paper.

#### References

- Andrady, A. L. (2011), Microplastics in the marine environment, *Mar. Pollut. Bull.*, 62(8), 1596–1605, doi:10.1016/j.marpolbul.2011.05.030.
- Barnes, D., and P. Milner (2005), Drifting plastic and its consequences for sessile organism dispersal in the Atlantic Ocean, *Mar. Biol. Berlin*, 146(4), 815–825, doi:10.1007/s00227-004-1474-8.
- Barnes, D., F. Galgani, R. C. Thompson, and M. Barlaz (2009), Accumulation and fragmentation of plastic debris in global environments, *Philos. Trans. R. Soc. B*, 364(1526), 1985–1998, doi:10.1098/rstb.2008.0205.
- Carpenter, E. J., and K. L. Smith (1972), Plastics on the Sargasso Sea surface, *Science*, 175(4027), 1240–1241, doi:10.1126/science.175.4027.1240.
- Colton, J. B., F. D. Knapp, and B. R. Burns (1974), Plastic particles in surface waters of the northwestern Atlantic, *Science*, 185(4150), 491–497, doi:10.1126/science.185.4150.491.
- Csanady, G. (2001), *Air-Sea Interaction*, 1st ed., 239 pp., Cambridge Univ. Press, Cambridge, U. K.
- D’Asaro, E. (2000), Simple suggestions for including vertical physics in oil spill models, *Spill Sci. Technol. Bull.*, 6(3–4), 209–211, doi:10.1016/S1353-2561(01)00039-1.
- Davison, P., and R. Asch (2011), Plastic ingestion by mesopelagic fishes in the North Pacific Subtropical Gyre, *Mar. Ecol. Prog. Ser.*, 432, 173–180, doi:10.3354/meps09142.

- Day, R. H., and D. G. Shaw (1987), Patterns in the abundance of pelagic plastic and tar in the north Pacific ocean, 1976–1985, *Mar. Pollut. Bull.*, 18(6), Suppl. 2, 311–316, doi:10.1016/S0025-326X(87)80017-6.
- de Boyer Montegut, C., G. Madec, A. S. Fischer, A. Lazar, and D. Iudicone (2004), Mixed layer depth over the global ocean: An examination of profile data and a profile-based climatology, *J. Geophys. Res.*, 109, C12003, doi:10.1029/2004JC002378.
- Guha, A. (2008), Transport and deposition of particles in turbulent and laminar flow, *Annu. Rev. Fluid Mech.*, 40(1), 311–341, doi:10.1146/annurev.fluid.40.1.11406.102220.
- Hopkins, T. L., R. C. Baird, and D. M. Milliken (1973), A messenger-operated closing trawl, *Limnol. Oceanogr.*, 18(3), 488–490, doi:10.4319/lo.1973.18.3.0488.
- International Pacific Research Center (2008), Tracking ocean debris, *IPRC Clim.*, 8(2), 1–3.
- Kantha, L. H., and A. C. Clayson (2004), On the effect of surface gravity waves on mixing in the oceanic mixed layer, *Ocean Modell.*, 6(2), 101–124, doi:10.1016/S1463-5003(02)00062-8.
- Komen, G. J., L. Cavaleri, M. Donelan, K. Hasselmann, S. Hasselmann, and P. A. E. M. Janssen (Eds.) (1996), *Dynamics and Modelling of Ocean Waves*, 532 pp., Cambridge Univ. Press, Cambridge, U. K.
- Kukulka, T., A. J. Plueddemann, J. H. Trowbridge, and P. P. Sullivan (2009), Significance of Langmuir circulation in upper ocean mixing: Comparison of observations and simulations, *Geophys. Res. Lett.*, 36, L10603, doi:10.1029/2009GL037620.
- Laist, D. W. (1987), Overview of the biological effects of lost and discarded plastic debris in the marine environment, *Mar. Pollut. Bull.*, 18(6), Suppl. 2, 319–326, doi:10.1016/S0025-326X(87)80019-X.
- Large, W. G., and S. Pond (1981), Open ocean momentum flux measurements in moderate to strong winds, *J. Phys. Oceanogr.*, 11, 324–336.
- Large, W. G., J. C. McWilliams, and S. C. Doney (1994), Oceanic vertical mixing: A review and a model with a nonlocal boundary layer parameterization, *Rev. Geophys.*, 32(4), 363–403, doi:10.1029/94RG01872.
- Law, K. L., S. Morét-Ferguson, N. A. Maximenko, G. Proskurowski, E. E. Peacock, J. Hafner, and C. M. Reddy (2010), Plastic accumulation in the North Atlantic Subtropical Gyre, *Science*, 329(5996), 1185–1188, doi:10.1126/science.1192321.
- Li, M., K. Zahariev, and C. Garrett (1995), Role of Langmuir circulation in the deepening of the ocean surface mixed layer, *Science*, 270, 1955–1957, doi:10.1126/science.270.5244.1955.
- Mato, Y., T. Isobe, H. Takada, H. Kanehiro, C. Ohtake, and T. Kaminuma (2001), Plastic Resin pellets as a transport medium for toxic chemicals in the marine environment, *Environ. Sci. Technol.*, 35(2), 318–324, doi:10.1021/es0010498.
- Maximenko, N., P. Niiler, L. Centurioni, M.-H. Rio, O. Melnichenko, D. Chambers, V. Zlotnicki, and B. Galperin (2009), Mean dynamic topography of the ocean derived from satellite and drifting buoy data using three different techniques, *J. Atmos. Oceanic Technol.*, 26(9), 1910–1919, doi:10.1175/2009JTECHO672.1.
- McWilliams, J. C., and P. P. Sullivan (2000), Vertical mixing by Langmuir circulations, *Spill Sci. Technol. Bull.*, 6(3–4), 225–237, doi:10.1016/S1353-2561(01)00041-X.
- Melville, W. K. (1996), The role of surface-wave breaking in air-sea interaction, *Annu. Rev. Fluid Mech.*, 28(1), 279–321, doi:10.1146/annurev.fl.28.010196.001431.
- Morét-Ferguson, S., K. L. Law, G. Proskurowski, E. K. Murphy, E. E. Peacock, and C. M. Reddy (2010), The size, mass, and composition of plastic debris in the western North Atlantic Ocean, *Mar. Pollut. Bull.*, 60(10), 1873–1878, doi:10.1016/j.marpolbul.2010.07.020.
- Skyllingstad, E. (2003), The effects of Langmuir circulation on buoyant particles, in *Handbook of Scaling Methods in Aquatic Ecology: Measurement, Analysis, Simulation*, edited by P. G. Strutton and L. Seuront, pp. 445–452, CRC Press, Boca Raton, Fla., doi:10.1201/9780203489550.ch28.
- Smith, J. A. (1992), Observed growth of Langmuir circulation, *J. Geophys. Res.*, 97(C4), 5651–5664, doi:10.1029/91JC03118.
- Smyth, W. D., E. D. Skyllingstad, G. B. Crawford, and H. Wijesekera (2002), Nonlocal fluxes and Stokes drift effects in the K-profile parameterization, *Ocean Dyn.*, 52(3), 104–115, doi:10.1007/s10236-002-0012-9.
- Stommel, H. (1949), Trajectories of small bodies sinking slowly through convection cells, *J. Mar. Res.*, 8(11), 24–29.
- Sudhakar, M., M. Doble, P. S. Murthy, and R. Venkatesan (2008), Marine microbe-mediated biodegradation of low- and high-density polyethylenes, *Int. Biodeterior. Biodegrad.*, 61(3), 203–213, doi:10.1016/j.ibiod.2007.07.011.
- Teuten, E., S. J. Rowland, T. S. Galloway, and R. C. Thompson (2007), Potential for plastics to transport hydrophobic contaminants, *Environ. Sci. Technol.*, 41(22), 7759–7764, doi:10.1021/es071737s.
- Teuten, E., et al. (2009), Transport and release of chemicals from plastics to the environment and to wildlife, *Philos. Trans. R. Soc. B*, 364(1526), 2027–2045, doi:10.1098/rstb.2008.0284.
- Thompson, R. C., Y. Olsen, R. P. Mitchell, A. Davis, S. J. Rowland, A. W. G. John, D. McGonigle, and A. E. Russell (2004), Lost at sea: Where is all the plastic?, *Science*, 304(5672), 838, doi:10.1126/science.1094559.
- Thorpe, S. A., T. R. Osborn, D. M. Farmer, and S. Vagle (2003), Bubble clouds and Langmuir circulation: Observations and models, *J. Phys. Oceanogr.*, 33(9), 2013–2031, doi:10.1175/1520-0485(2003)033<2013:BCALCO>2.0.CO;2.
- Titmus, A. J., and D. K. Hyrenbach (2011), Habitat associations of floating debris and marine birds in the north east Pacific Ocean at coarse and meso spatial scales, *Mar. Pollut. Bull.*, 62(11), 2496–2506, doi:10.1016/j.marpolbul.2011.08.007.
- Webb, H., R. Crawford, T. Sawabe, and E. Ivanova (2009), Poly (ethylene terephthalate) polymer surfaces as a substrate for bacterial attachment and biofilm formation, *Microbes Environ.*, 24(1), 39–42, doi:10.1264/jsm2.ME08538.
- Wessel, P., and W. H. F. Smith (1998), New, improved version of generic mapping tools released, *Eos Trans. AGU*, 79(47), 579, doi:10.1029/98EO00426.
- Wilber, R. J. (1987), Plastic in the North Atlantic, *Oceanus*, 30(3), 61–68.
- Wong, C. S., D. R. Green, and W. J. Cretney (1974), Quantitative tar and plastic waste distributions in Pacific Ocean, *Nature*, 247(5435), 30–32, doi:10.1038/247030a0.

T. Kukulka, School of Marine Science and Policy, College of Earth, Ocean, and Environment, University of Delaware, 211 Robinson Hall, Newark, DE 19716, USA. (kukulka@udel.edu)

K. L. Law and S. Morét-Ferguson, Sea Education Association, PO Box 6, Woods Hole, MA 02543, USA.

D. W. Meyer, Eckerd College, 4200 54th Ave. South, St. Petersburg, FL 33711, USA.

G. Proskurowski, School of Oceanography, University of Washington, Box 357940, Seattle, WA 98195, USA. (giora@uw.edu)